Exploring constraints of Dirac fields on gravitational wave dephasing

P. R. Dhungel*, S. K. Sharma and U. Khanal*****

*Department of Physics, St. Xavier's College, Tribhuvan University, Kathmandu, Nepal.

** B. P. Koirala Memorial Planetarium, Observatory and Science Museum Development Board, MoEST, Kathmandu, Nepal.

*** Professor of Physics, Mid – Baneshwor, Kathmandu, Nepal.

Abstract: Modern gravitational-wave (GW) parameter estimation greatly depends on highly precise vacuum templates framed in General Relativity which assume that compact binaries coalesce in an absolute vacuum. But actual astrophysical backgrounds possess dense matter distributions, including baryonic accretion disks, dark matter halos, and background cosmic Dirac fields. In this paper, the quantitative impact of external matter fields on the inspiral phase of compact binaries has been evaluated. Focus is specifically on a black hole binary ($36\ \mathrm{M}_{\odot} + 29\ \mathrm{M}_{\odot}$) like GW150914. We model the dissipative corrections introduced by gravitational drag (dynamical friction) at the negative Post-Newtonian (-2PN) order in natural geometric units (G = c = 1).

Using standard analytical implementations and numerical simulations, the phase deviation $\Delta\Psi(f)$ has been mapped across the ground-based (aLIGO) observation window (30 - 100 Hz). The indication of the findings is that for cosmic localized Dirac field configurations (ranging from $\rho \sim 10^{-50}\ \mathrm{m}^{-2}$ to $10^{-26}\ \mathrm{m}^{-2}$), the cumulative phase shifts at 30 Hz remain entirely suppressed ($< 10^{-15}$ rad). This validates the fact that current ground-based observing runs operating within the "Vacuum Limit," leave standard general relativity parameter estimations unperturbed while imposing the constraints will be necessary for future multi-band space missions.

Keywords: Dirac fields; Gravitational Wave; Dephasing; LIGO; Inspirals.

Introduction

From the detection of GW150914 by the Laser Interferometer Gravitational-Wave Observatory (LIGO), the important era of precision gravitational-wave physics began and then the series of observation runs catalogued in the Gravitational-Wave Transient Catalogues (GWTC-1 through GWTC-3) have made the tests of general relativity possible in the strong-field, highly dynamical regime[1,2,3]. Experimental strain data matching against the numerical relativity and Post-Newtonian (PN) waveforms have enabled the systematic extraction of parameters such as component masses and spins with sub-percent level of accuracy[4, 5].

Although we have achieved these successes, standard frameworks are built assuming that the merging compact binaries are isolated in absolute vacuums. But in realistic astrophysical contexts, black hole (BH) binaries are embedded within active galactic nuclei (AGNs), circum-binary accretion disks, or local dark matter spikes. While the satellite component of the binary sweeps through the external matter distribution, it experiences non-gravitational and environmental forces that distort its clean geodesic trajectory. The adiabatic perturbations thus produced accompany the emitted gravitational waveform that may bias the parameter estimation or give false signal

Author for correspondence: Prem Raj Dhungel, Department of Physics , St. Xavier's College, Tribhuvan University, Kathmandu, Nepal.
Email: premrd@sxc.edu.np; https://orcid.org/0000-0002-5044-8423
Received: 1 June, 2026; Received in revised form: 7 June, 2026; Accepted: 14 June, 2026.
Doi: https://doi.org/10.3126/sw.v19i19.95903

of violation of general relativity[6, 7].

In this paper, we have carried out an analysis of environmental dephasing during the binary inspiral. It is based on the analytical framework established by Barausse, *et. al.*[8] where we examine how viscous and gravitational drag forces break the vacuum degeneracy.

Since all matter is ultimately fermionic(unless the complete knowledge of dark matter reveals something else), the behaviour of a Dirac field and the matter fields in general, must have profound role and consequences in the expanding Universe.[9,10,11,12]. So, we have used Dirac field conditions explored in and estimated from our previous work[13] as the environmental profiles. To determine where the environmental interactions cross the threshold of observational detectability, we check across multiple orders of the geometric density.

In the next section, we briefly discuss about the framework and waveform-modelling followed by the method of computation. Then we present and compare the data thus obtained and then carry out the discussion and conclusion.

Framework and Waveform-modelling

For a compact binary system, how the orbital evolution takes place is described by the following equation where the energy radiated away through gravitational waves and absorbed by the surrounding medium is equated to the loss of orbital energy:

$$\frac{\mathrm{dE_{orb}}}{\mathrm{dt}} = -\dot{E}_{GW} - \dot{E}_{env} \qquad \ldots(1)$$

In natural geometric units, G = c = 1, mass (M) will take dimension of length (meter), and density (ρ) the dimension of curvature (i.e., meter^{-2}). In the leading Newtonian order, the GW energy flux carried away is given by:

$$\dot{E}_{GW} = \frac{32}{5}\nu^2\frac{M_{\text{tot}}^5}{r^5} \qquad \ldots(2)$$

where $M_{\text{tot}} = m_1 + m_2$ is the total mass, $\nu = m_1 m_2/M_{\text{tot}}^2$ is the symmetric mass ratio, and r is the orbital separation, $m_1$and m_2 being the masses of the two components of a binary.

When the binary moves through a homogeneous background of density ρ, a gravitational wake is generated behind its path which exerts a retarding force called dynamical friction (DF) dissipating the energy. This energy flux can be written as

$$\dot{E}_{env} = \dot{E}_{DF} = F_{\text{DF}} \cdot v_{\text{K}} \qquad \ldots(3)$$

where v_{K}, given by $\sqrt{M_{\text{tot}}/r}$, is the local Keplerian velocity, and F_{DF} is the drag force given by:

$$F_{\text{DF}} = \frac{4\pi\rho m_{\text{sat}}^2}{v_{\text{K}}^2} I \qquad \ldots(4)$$

Here, I represents the modified Coulomb logarithm. Since DF depends directly on the background density ρ and becomes stronger at larger separations (where velocities go lower but interaction times become longer), it changes the phase evolution at a low Post-Newtonian (PN) order and hence enters the waveform phase at the **-**2PN order compared to the leading-order vacuum term.

The absolute frequency-domain phase modification $\Delta\Psi(f)$ induced by this **-2PN** gravitational drag sweep can be written analytically by using the stationary phase approximation (SPA)

$$\Delta\Psi(f) = \frac{25}{32}\pi M_{\text{tot}}\rho \cdot v^{-11} \qquad \ldots(5)$$

where $v = (\pi M_{\text{tot}} f)^{1/3}$ denotes the dimensionless orbital velocity parameter, and f is the GW frequency in geometric units (m^{-1}). Due to this steep negative dependence on velocity (v^{-11}), i.e., $f^{-11/3}$ in terms of frequency, the dephasing grows exponentially at lower frequencies (i.e., f→0). So, it is a very sensitive investigation for early stage inspirals.

We have considered, for simplicity, uniform light neutrino background density $\rho \sim 10^{-31}\ kg/m^3$ estimated from our earlier work[13] (which obtained co-moving number density to be, $na^3 \approx 0.0828$).

Computational Methodology

To explore the actual observational impact of this dephasing, we carried out a numerical simulation in Python replicating a GW150914 base profile ($m_1 = 36.0 M_{\odot}$, $m_2 = 29.0 M_{\odot}$).[14]

The frequency sweep[15] was kept between $f_{\text{start}} = 30$ Hz and $f_{\text{end}} = 100$ Hz. Converting this into geometric frequency using $f_{\text{geo}} = f_{\text{SI}}/c$, the starting frequency comes to be $f_{\text{start}} \approx 1.00 \times 10^{-7}$ m^{-1}.

We used a logarithmic geometric density matrix spanning seven orders of magnitude, ranging from a very small cosmological cosmic field baseline ($\rho \sim 1.0 \times 10^{-50}$m^{-2}) up to denser environmental limits ($\rho \sim 1.0 \times 10^{-2}$). The modification. It is noteworthy that even at the highest evaluated background density ($\rho = 1.00 \times 10^{-26}$ m^{-2}), the cumulative dephasing comes to be very small: 8.84×10^{-16} rad.

In Fig.-1, these environmental trajectories have been plotted on a multi-scale logarithmic visual scale (loglog). They distinctly split into parallel lines. However, in the active ground-based band (30 Hz to 100 Hz), these trajectories are

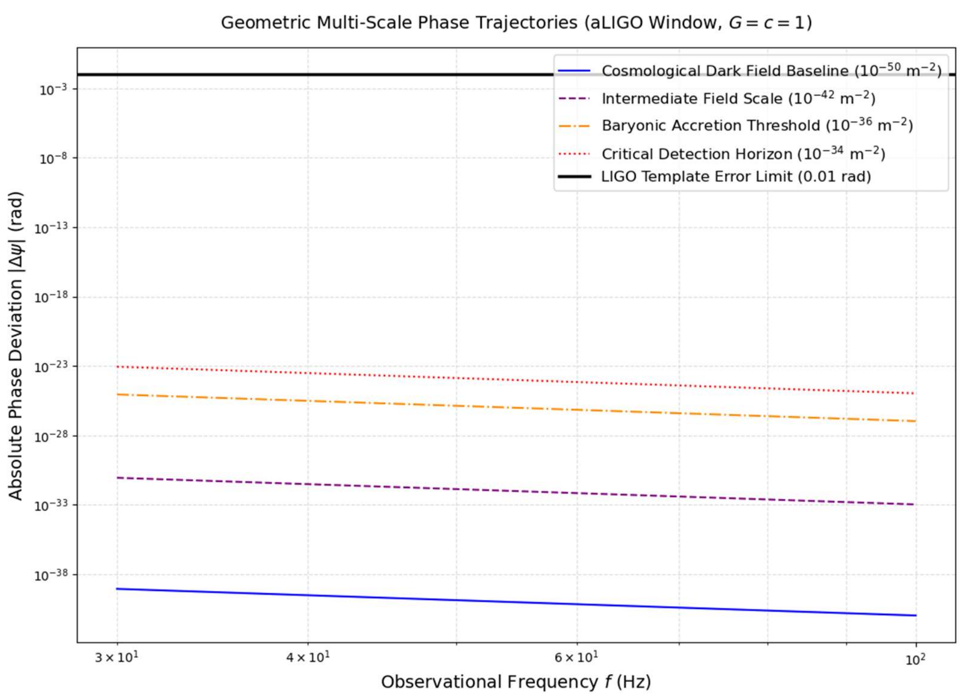

Figure 1: Environmental trajectories plotted on a multi-scale logarithmic visual scale (loglog) for eLIGO window in natural geometric units (G = c = 1): Absolute phase deviation ($|\Delta\Psi|$) against the observation frequency in the band 30 – 100 Hz. The thick solid line on the top is LIGO Template Error limit (0.01 rad) and the dotted line below it is the critical detection horizon (10^{-34} m^{-2}). With reference to these, the solid line at the lowest level is for the Cosmological Dark field baseline (10^{-50} m^{-2}). The two lines above this the dashed and dot-dashed are for Baryonic Accretion Threshold (10^{-36} m^{-2}) and Intermediate Field scale (10^{-42} m^{-2}) respectively. The absolute phase shift drops by a factor of approximately 84 as the binary accelerates from 30 Hz to 100 Hz. Even if an 84-fold drop is physically significant, it visually appears as a uniform horizontal profile while mapping against such a massive vertical scale. This physically indicates that during a fraction of a second before a ground-based merger, the -2PN environmental drag acts effectively as a very small and static phase offset rather than a highly dynamic evolution.

absolute phase deviations thus obtained were compiled and evaluated against a standard template mismatch sensitivity threshold of $\Delta\Psi \sim 0.01$ rad.

Data comparison for Validation

The numerical results obtained across the geometric density sweep at starting frequency 30Hz are given in Table 1. The results explicitly show a linear scaling between the environmental matter background and the resulting phase

almost flat against the frequency axis. This profile comes directly from the extreme dynamic scale required to plot the values, which spans over 24 orders of magnitude vertically. The $f^{-11/3}$ power-law makes the absolute phase shift drop by a factor of approximately 84 as the binary accelerates from 30 Hz to 100 Hz. Even if an 84-fold drop is physically significant, it visually appears as a uniform horizontal profile while mapping against such a massive vertical scale. This physically indicates that during a fraction of a second before a ground-based merger, the -2PN environmental

Table 1: Natural Geometric Phase Trajectories ($f = 30$ Hz, $M_{\text{tot}} = 96,005$ m).

Geometric Density ρ (m^{-2})	Absolute Phase Shift $\|\Delta\Psi\|$ (rad)	Observational Status
1.00×10^{-50}	8.84×10^{-40}	Absolute Vacuum Baseline
1.00×10^{-46}	8.84×10^{-36}	Absolute Vacuum Baseline
1.00×10^{-42}	8.84×10^{-32}	Absolute Vacuum Baseline
1.00×10^{-38}	8.84×10^{-28}	Absolute Vacuum Baseline
1.00×10^{-34}	8.84×10^{-24}	Absolute Vacuum Baseline
1.00×10^{-30}	8.84×10^{-20}	Absolute Vacuum Baseline
1.00×10^{-26}	8.84×10^{-16}	Absolute Vacuum Baseline

.

drag acts effectively as a very small and static phase offset rather than a highly dynamic evolution.

Results and Discussion

As shown in Table 1, the extreme suppression of the phase values gives an understanding of the observational constraints of ground-based GW networks. The observation window for stellar-mass black holes is extremely small for detectors like Advanced LIGO, Advanced Virgo, and KAGRA. A binary system like GW150914 sweeps through the highly sensitive band of 30 – 100 Hz in a very small duration merely a few seconds. This rapid dominating radiation reaction forces overshadow the minor drag contributions of the environmental medium.

As a result, cosmological backgrounds like the uniform quantized Dirac field distributions derived from momentum expectations are negligible and hence hidden within the instrumentation noise floor. Thus, it is confirmed from the data that standard vacuum template banks are still strong enough for current ground-based catalogues and hence it ensures that environmental systematic biases do not spoil current tests of general relativity.

However, the dependence on steep power-law $f^{-11/3}$ changes this perspective when moving to space-based laser interferometers like the Laser Interferometer Space Antenna (LISA). While operating in the milli-Hertz band (10^{-4} Hz $\rightarrow 10^{-2}$ Hz), LISA's targets are massive and intermediate-mass black hole binaries years before their final merger. In this low-frequency range, the velocity parameter v drops significantly, making the v^{-11} multiplier scale upward by 10 to 15 orders of magnitude. The space-borne architectures with observation windows of several years will have a unique capacity to amplify the negative PN interactions. This will enhance future space-based detectors to highly sensitive instruments with the capability of probing subtle, low-density cosmic fields (like Dirac fields) that are entirely invisible to ground-based interferometers.

Conclusion

It is seen from this study that the -2PN dephasing induced by dynamical friction gives an explicit diagnostic distinction between various GW observation bands. By applying the analytical framework in the natural geometric unit system ($G = c = 1$), it is shown that for localized cosmic backgrounds ranging up to $\rho \sim 10^{-2}$ m^{-2}, the dephasing in ground-based instruments is entirely negligible. This means that the pure vacuum general relativity templates are valid for current interferometers like Advanced LIGO.

However, because of the power-law divergence of background drag at low frequencies, these feeble quantum field signatures scale upward significantly within the milli-Hertz band. This unfolds the importance and long-term potential of space-based missions like LISA to utilize early inspiral physics as a means for imposing constraints on alternative dark matter and cosmic field environments.

Data Availability Statement

The empirical GW strain data utilized as the observational baseline for this study (especially the event GW150914) are publicly available through the Gravitational Wave Open Science Centre (GWOSC). This is maintained by the Lars Network, the LIGO Laboratory, and the Virgo/KAGRA Collaborations. The raw and down-sampled data vectors, calibration files, and baseline data-quality segments can be accessed freely online at: https://gwosc.org (or through https://doi.org/10.7935/K5MW2F2W). The numerical data sweeps and tracking code compiled within the natural geometric framework (G = c = 1) during this analysis are available from the corresponding author upon reasonable request.

References

1. Abbott, B. P., et al. 2016. Observation of Gravitational Waves from a Binary Black Hole Merger. *Physical Review Letters*. **116**(6)**:** 061102.
2. Abbott, R., et al. 2021. GWTC-3: Compact binary coalescences observed by LIGO and Virgo during the second part of the third observing run. *arXiv preprint arXiv:2111.03606*.
3. Amaro-Seoane, P., et al. 2017. Laser interferometer space antenna (LISA mission blueprint). *arXiv preprint arXiv:1702.00786*.
4. Yunes, N., Yagi, K. & Pretorius, F. 2016. *Theoretical Physics Implications of the Binary Black-Hole Mergers GW150914 and GW151226.* Physical Review D. **94**(8): 084002. (arXiv:1603.08955)
5. Blanchet, L. 2014. Gravitational radiation from post-Newtonian sources and binary systems. *Living Reviews in Relativity*. **17**(1): 2.
6. Ostriker, E. C. 1999. Dynamical friction in a gaseous medium. *The Astrophysical Journal*. **513**(1): 252. Doi: https://doi.org/10.1086/306858
7. Chandrasekhar, S. 1943. Dynamical friction. I. General considerations: the coefficient of fluctuation. *The Astrophysical Journal*. **97**: 255. Doi: https://doi.org/10.1086/144517
8. Barausse, E., Cardoso, V. & Pani, P. 2014. Can environmental effects spoil precision gravitational-wave astrophysics? *Physical Review D*. **89**(10): 104059. Doi: https://doi.org/10.1103/physrevd.89.104059
9. Lesgourgues, J. & Pastor, S. 2006. Massive neutrinos and cosmology. Physics Reports. **429**(6): 307-379. Doi: https://doi.org/10.1016/j.physrep.2006.04.001
10. Macedo, C. F., et al. 2013. Into the lair: gravitational-wave signatures of dark matter. *The Astrophysical Journal*. **774**(1): 48. Doi: https://doi.org/10.1088/0004-637x/774/1/48
11. Bond, J. R., Efstathiou, G. & Silk, J. 1980. Massive neutrinos and the formation of galaxies. *Physical Review Letters*. **45**(24): 1980. Doi: https://doi.org/10.1103/physrevlett.45.1980
12. Parker, L. 1969. Quantized fields and particle creation in expanding universes. I. *Physical Review*. **183**(5): 1057. Doi: https://doi.org/10.1103/physrev.183.1057
13. Dhungel, P. R. & Khanal, U. 2013. Dirac field in FRW spacetime: current and energy momentum. *Chinese Journal of Physics*. **51**(5): 882-902.
14. Cornish, N. J. & Littenberg, T. B. 2015. BayesWave: bayesian inference for gravitational wave bursts and instrument glitches. *Physical Review D*. **91**(12): 122004. Doi: https://doi.org/10.1088/0264-9381/32/13/135012
15. Kavanagh, B. J., et al. 2020. Detecting dark matter spikes around intermediate mass black holes with LISA. *Physical Review D*. **102**(8): 083014. Doi: https://doi.org/10.1103/physrevd.102.083006

[redacted]